# Observation of the Second Tensor Nonet with the L3 Experiment

Schegelsky V.A., Sarantsev A.V., Nikonov V.A., Anisovich A.V., Levtchenko M.P.
*Petersburg Nuclear Physics Institute, Gatchina, Russia*

The data on the reactions $\gamma\gamma \to \pi^+\pi^-\pi^0$ and $\gamma\gamma \to K^0_S K^0_S$ are collected by the L3 detector at LEP. In the reaction $\gamma\gamma \to \pi^+\pi^-\pi^0$ a strong signal consistent with the first radial excitation of the isovector tensor state, $a_2(1700)$ , is observed with the mass $M = (1722 \pm 9 \pm 8)$ MeV and the width $\Gamma = (336 \pm 20 \pm 20)$ MeV. The mass spectrum of the $K^0_S K^0_S$ is dominated by the formation of tensor mesons. The signal at (1700-1800) MeV region is proved to be due to a new state - the tensor meson $f_2(1750)$ with mass $M = (1755 \pm 10)$ MeV and width $\Gamma = (67 \pm 12)$ MeV. The $f_2(1750)$ state forms the second tensor nonet together with $f_2(1560)$ and $a_2(1700)$. In the $SU(3)$ based analysis the present data allows us to determine mixing angles of tensor nonets with good accuracy.

The L3 detector on Electron Collider of CERN is an universal set up [1] to detect particles with momentum up to 100 GeV. Colliding electron beams each with a 100 GeV momentum are very powerful source of 'colliding quasi-real photons'. These photons then can produce hadronic final states with an effective mass of several GeV. The very precise central tracker and BGO electromagnetic calorimeter of L3 provide excellent measurements even at very low energies.

The $\gamma\gamma$ collision reactions is a powerful tool for the investigation of meson states. It is especially valuable that the data not only supply the information about masses and widths of resonances but also about their couplings to the gamma-gamma channel which can be directly calculated in the framework of quark models.

## 1 The selection of the $\gamma\gamma \to \pi^+\pi^-\pi^0$ data

The selection of two-photon reaction $e^+e^- \to e^+e^-\pi^+\pi^-\pi^0$ requires in the final state two charged particles and two gammas with an effective mass close to $\pi^0$ mass. The background can be evaluated from the side bands of the $\pi^0$ mass distribution. The 17124 events are selected with cut $P_t \leq 0.1$ GeV. The $\pi^+\pi^-\pi^0$ mass distribution shown in Fig. 1a, is dominated by the production of the $a_2(1320)$ state. There is a shoulder in the mass region 1.6-1.8 GeV. The main signal in the $\pi^\pm\pi^0$ mass spectrum (see Fig. 1b), is due to the production of $\rho(770)$. There is very little structure in the region above 1 GeV and almost no events higher than 1.5 GeV. The $\pi^+\pi^-$ mass distribution is shown in Fig. 1c. There is no sharp structure here at low $\gamma\gamma$ energies but at high energies the signal from the $f_2(1275)$ is clearly seen (see Fig. 1d).

## 2 Analysis of the reaction $\gamma\gamma \to \pi^+\pi^-\pi^0$

Resonances produced in $\gamma\gamma$ channel should have the positive C-parity. A produced $q\bar{q}$ state with negative G-parity (which is defined by three pion final state) has isospin 1. To describe three

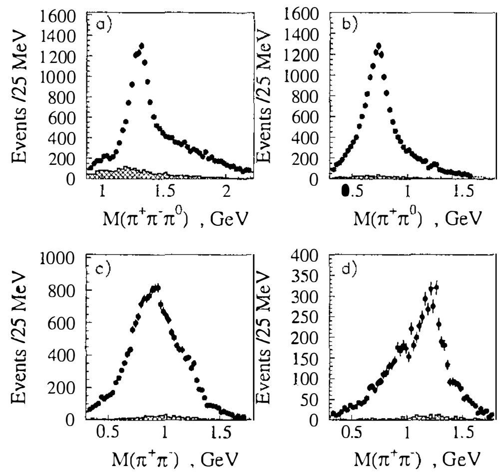


Figure 1: Mass spectra a) $M(\pi^+\pi^-\pi^0)$; b) $M(\pi^\pm\pi^0)$; c) $M(\pi^+\pi^-)$; d) $M(\pi^+\pi^-)$ with 3 pion mass higher than 1.5 GeV; The background, estimated from the side bands of the $\pi^0$ meson distribution, is shown as a shaded area.

Table 1: Mass, width and the product of $\Gamma_{\gamma\gamma}$ times $Br(3\pi)$ for the observed resonances. The name of the resonances is taken from Ref.[5]

| Resonance | M (MeV) | $\Gamma$ (MeV) | $\Gamma_{\gamma\gamma}Br(3\pi)$ (KeV) |
|---|---|---|---|
| $a_2(1320)$ | $1300 \pm 2 \pm 2$ | $117 \pm 6 \pm 10$ | $0.65 \pm 0.02 \pm 0.02$ |
| $a_2(1700)$ | $1722 \pm 9 \pm 8$ | $336 \pm 20 \pm 20$ | $0.37^{+0.12}_{-0.08} \pm 0.10$ |
| $a_2(2030)$ | $2050 \pm 10 \pm 10$ | $190 \pm 22 \pm 30$ | $0.11 \pm 0.04 \pm 0.05$ |
| $\pi(1300)$ | $1345 \pm 8 \pm 10$ | $260 \pm 20 \pm 30$ | $\leq 0.8 (95\% CL)$ |
| $2^{-+}$ | $1860 \pm 12 \pm 10$ | $352 \pm 30 \pm 40$ | $0.15 \pm 0.03 \pm 0.05$ |
| $\pi_2(1670)^*$ | 1670 | 260 | $\leq 0.1 (95\% CL)$ |

* - the $2^{-+}$ parameters are fixed as $\pi_2(1670)$ with values taken from Ref.[5].

pion production data we perform the number of fits with different combinations of resonances and background. To describe the two-pion masses and all angular distributions in the whole energy interval we need three tensor states $a_2(1320)$, $a_2(1700)$ and $a_2(2030)$, a pseudoscalar state which can be identified with the $\pi(1300)$ and a $2^{-+}$ state. This hypothesis gives a good description of the $\pi^+\pi^-\pi^0$ mass spectrum, as shown in Fig. 2.

The masses, widths and resonance $\gamma\gamma$ widths are listed in Table 1. The contribution of the resonances into total cross section is shown in Fig. 2.

## 3 Analysis of the reaction $\gamma\gamma \to K_sK_s$

The selection of $\gamma\gamma \to K_sK_s$ events is based on the $K_s$ decay into $\pi^+\pi^-$. The $K_s$ are identified by the secondary vertex reconstruction. The $K_s$ mass resolution was found to be $\sigma = 9.5 \pm .2$ MeV. With our selection criteria the 870 events have been found. The background due to misidentified $K_s$ pairs is estimated to be less than 10%.

Only $J^{PC} = (2n)^{++}$ states decay into $K_sK_s$ system. For quasi-real photons only one com-

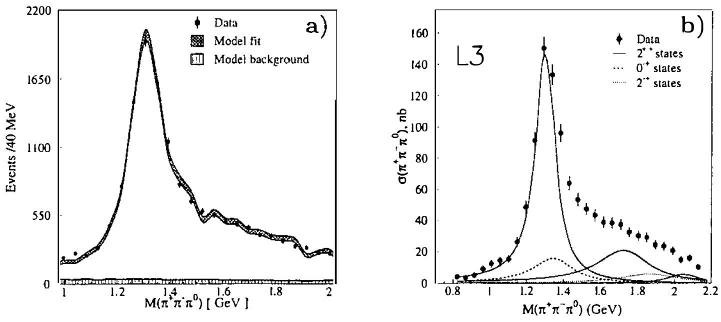


Figure 2: The $\pi^+\pi^-\pi^0$ mass distribution: a) the data (full points ) and the result of the partial wave analysis fit ( fit curve with corridor of statitical errors). b) Contribution of the resonances to the cross section: the full curves correspond to three $2^{++}$ states, the dashed curve to the $0^{-+}$ and dotted curve to the $2^{-+}$ contributions.

bination of spin and angular momentum operators forms $0^{++}$ state: ${}^{2s+1}L_J = {}^1S_0$. The $2^{++}$ partial wave can be produced from $\gamma\gamma$ states: ${}^1D_2$ and ${}^5S_2$. A $4^{++}$ state is from ${}^1G_4$ and ${}^5D_4$.

The prediction from quark model calculation which was confirmed from investigation of many $\gamma\gamma$ production reactions is that $\sigma({}^5S_2) \sim 6\sigma({}^1D_2)$ [2]. Indeed the angular distribution follows very close to the $(1-\cos^2\Theta)^2$ shape which corresponds to ${}^5S_2$ partial wave. However due to our acceptance which falls rapidly at large $\cos\Theta$ it is nevertheless difficult to distinguish between a tensor and a scalar state.

There is no doubt about the structure of the $K_sK_s$ mass distribution below 1600 MeV: the spectrum is defined by the destructive interference between the $a_2(1320)$ and $f_2(1270)$ states and a clear signal from $f_2(1525)$. The description with such components is shown in Fig. 3a.

A contribution from $a_0(980)/f_0(980)$ states is present in the data a bit above $K\bar{K}$ threshold. The $a_0(980)$ state is parametrised with Flatté form with coupling to $\pi\eta$ and $K\bar{K}$ channels given in [3]. Another contribution at high energies comes from $4^{++}$ partial wave. The fit points out to a narrow state with mass $(2150 \pm 30)$ MeV and width $(50 \pm 20)$ MeV. This can be an indication of a $s\bar{s}$ $4^{++}$ state. However on the basis of the present statistics, we can not exclude a statistical fluctuation.

The fit with all above mentioned components is shown in Fig. 3b and it fails to reproduce a structure at 1700-1800 MeV. The description of the data with a scalar state fitted with free mass and width is shown in Fig. 3c. If mass is fixed to parameters from [4] $M = 1740$ MeV we obtain the description shown in Fig. 3d.

The main problem in fits with $f_0$ states is that there is no way to reproduce the dip in the 1700 MeV region and the slope above 1800 MeV. The $f_0$ and $f_2$ contributions do not interfere in the total cross section which leads to filling the dip in the region 1700 MeV.

With a tensor state in the region 1750 MeV we immediately find good description of the mass spectrum (Fig. 3e)). The mass of the state is found to be $(1755 \pm 10)$ MeV and the width $(67 \pm 12)$ MeV. The fit describes well the dip between $f_2'(1525)$ and $f_2(1750)$ states with a natural interference between two tensor states.

The meson states consisting of light quarks $n = u, d$ and strange quarks $s$ form meson nonet: octet and singlet state. The members of the first tensor nonet are well known and we assum that $a_2(1700)$, $f_2(1560)$ and observed $f_2(1750)$ forms the second tensor nonet. The coupling of $f_2(1560)$ and $a_2(1700)$ is known from the analysis of $p\bar{p}$ annihilation data. Then free parameters for this nonet are the mixing angle and the mass and total width of $f_2(1750)$. Under this

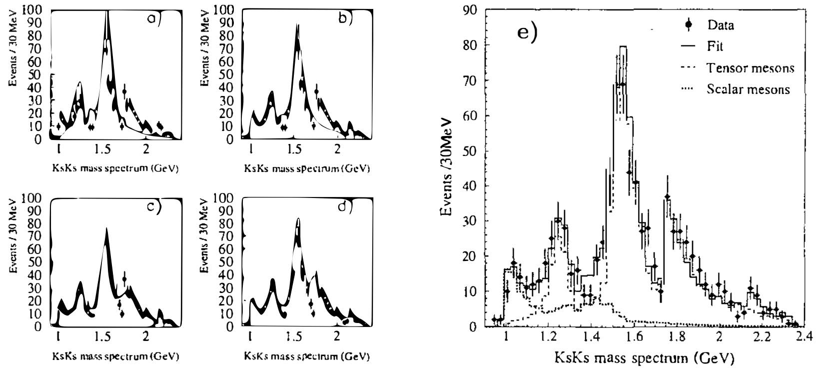


Figure 3: The description of the data: a) with the first tensor nonet states only; b) with added low mass scalar states and $4^{++}$; contributions c) (b) plus $f_0(1710)$ state with free parameters; d) same as (c) but the mass and width of $f_0(1710)$ is fixed from [4]; e) The description of the data with $f_2(1750)$ state.

assumption we are able to reproduce the description with the same quality as in the free fit with free parameters.

## 4 Summary

The $a_2(1720)$ state is discovered in the L3 data. The gamma-gamma partial width of tensor isovector resonances are defined with a good accuracy. The data on $\gamma\gamma \to K_s K_s$ shows a NEW narrow state at 1750 MeV with spin 2. SU(3) based calculations show that this state can be naturally considered as a member of the second tensor nonet.

## References


1. L3 Coll., B. Adeva et al., Nucl. Instr. and Meth. **A 289** (1990) 35;
   M. Acciarri et al., Nucl. Instr. and Meth. **A 351** (1994) 300;
   M. Chemarin et al., Nucl. Instr. and Meth. **A 349** (1994) 345;
   A. Adam et al., Nucl. Instr. and Meth. **A 383** (1996) 342.
2. A.V. Anisovich, V.V. Anisovich, M.A. Matveev, V.A. Nikonov. Apr 2002. 37pp. "Two photon partial widths of tensor mesons", hep-ph/0204330
3. V. V. Anisovich and A. V. Sarantsev, Eur. Phys. J. A **16** (2003) 229, hep-ph/0204328.
4. J.Z. Bai et al., (BES collaboration), Phys. Lett. B472 (2000) 207.
5. K. Hagiwara et al. (Particle Data Group), Phys. Rev. D **66** (2002) 1.